ACS APPLIED MATERIALS & INTERFACES

Research Article

www.acsami.org

Bioinspired Collagen/Glycosaminoglycan-Based Cellular Microenvironments for Tuning Osteoclastogenesis

Sandra Rother,[†] Juliane Salbach-Hirsch,[‡] Stephanie Moeller,[§] Thomas Seemann,[§] Matthias Schnabelrauch,[§] Lorenz C. Hofbauer,[‡] Vera Hintze,[†] and Dieter Scharnweber*[,†]

[†]Institute of Materials Science, Max Bergmann Center of Biomaterials, Technische Universität Dresden, Budapester Straße 27, 01069 Dresden, Germany

[‡]Division of Endocrinology, Diabetes, and Bone Diseases of Medicine III, Technische Universität Dresden Medical Center, Fetscherstraße 74, 01307 Dresden, Germany

[§]Biomaterials Department, INNOVENT e.V., Prüssingstraße 27 B, 07745 Jena, Germany

ABSTRACT: Replicating the biocomplexity of native extracellular matrices (ECM) is critical for a deeper understanding of biochemical signals influencing bone homeostasis. This will foster the development of bioinspired biomaterials with adjustable bone-inducing properties. Collagen-based coatings containing single HA derivatives have previously been reported to promote osteogenic differentiation and modulate osteoclastogenesis and resorption depending on their sulfation degree. However, the potential impact of different GAG concentrations as well as the interplay of multiple GAGs in these coatings is not characterized in detail to date. These aspects were addressed in the current study by integrating HA and different sulfate-modified HA derivatives (sHA) during collagen in vitro fibrillogenesis. Besides cellular microenvironments with systematically altered single-GAG concentrations, matrices containing both low and high sHA (sHA1, sHA4) were characterized by biochemical analysis such as agarose gel electrophoresis, performed for the first time with sHA derivatives. The morphology and composition of the collagen coatings were altered in a GAG sulfation- and concentration-dependent manner. In multi-GAG microenvironments, atomic force microscopy revealed intermediate collagen fibril structures with thin fibrils and microfibrils. GAG sulfation altered the surface charge of the coatings as demonstrated by ζ-potential measurements revealed for the first time as well. This highlights the prospect of GAG-containing matrices to adjust defined surface charge properties. The sHA4- and the multi-GAG coatings alike significantly enhanced the viability of murine osteoclast-precursor-like RAW264.7 cells. Although in single-GAG matrices there was no dose-dependent effect on cell viability, osteoclastogenesis was significantly suppressed only on sHA4-coatings in a dose-dependent fashion. The multi-GAG coatings led to an antiosteoclastogenic effect in-between those with single-GAGs which cannot simply be attributed to the overall content of sulfate groups. These data suggest that the interplay of sGAGs influences bone cell behavior. Whether these findings translate into favorable biomaterial properties needs to be validated in vivo.

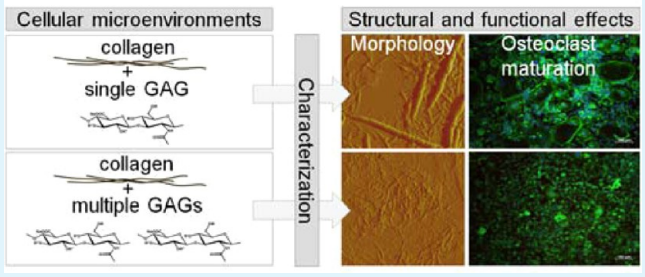

KEYWORDS: *hyaluronic acid/hyaluronan (HA) sulfate, collagen, extracellular matrix (ECM), biomimetic material, osteoclast, atomic force microscopy (AFM)*

1. INTRODUCTION

In light of a prolonged life expectancy, the need for biomaterials that govern bone regeneration is increasing. The clinical necessity of further advancing bone engineering is highlighted by the fact that, out of the 4 million operations performed annually, implant failure or delayed healing may occur in up to 5−20% of all fractures.[1] In future, especially the development of functional materials toward patient-specific needs will even become more important as the individual bone formation potential can fundamentally vary by person with respect to risk factors (e.g., diabetes), age, and comorbidities.[2]

Bone homeostasis requires a well-orchestrated signaling network between bone-forming osteoblasts and bone-resorbing osteoclasts. The structure and composition of the extracellular matrix (ECM) as the surrounding microenvironment of cells in tissues plays a crucial role in a variety of biological processes.[3] Therefore, the development of biomaterials mimicking important ECM features is a promising approach to be utilized for tissue regeneration.[4] Collagen (coll) type I is the major organic component of bone ECM providing physical structure as well as binding sites for glycosaminoglycans (GAGs) and facilitating cell adhesion through distinct amino acid sequences.[5,6] Proteoglycans are further important ECM components with naturally sulfated GAG chains as their

Received: September 8, 2015
Accepted: October 9, 2015
Published: October 9, 2015

DOI: 10.1021/acsami.5b08419
ACS Appl. Mater. Interfaces 2015, 7, 23787−23797

functional components. GAGs are complex linear polysaccharides, able to interact, bind, concentrate, and sequester biological mediator proteins like growth factors and cytokines, playing a key role in the regulation of bone formation and remodeling.[7−11] In bone, the ECM contains a mixture of GAGs with 90% chondroitin-4 sulfate and small amounts of hyaluronan (HA), dermatan sulfate, and chondroitin-6 sulfate (CS).[12]

Therefore, native GAGs as well as composites of native GAGs and coll have been studied for more than 40 years for various biomedical applications like skin, bone, peripheral nerve, and cartilage tissue regeneration.[13−19] However, because of the variations in the carbohydrate backbone and the sulfation pattern of these GAGs the information on cell interaction with the matrix is limited. Furthermore, proteoglycans and even naturally high-sulfated GAGs like heparan sulfate are limited in their utility for in vivo applications in coll-based coatings due to their batch-to-batch variety, insufficient availability, and immunogenic potential of the core protein of proteoglycans.[20]

HA is a promising tool for tissue engineering applications because its defined and regular molecule structure, good biotechnological availability, and low immunogenicity.[20,21] The chemical sulfation of hyaluronan (sHA) leads to polysaccharides with defined sulfation degree and pattern as well as molecular weight. In general, the increasing incorporation of sulfate residues into the carbohydrate backbone leads to a strong increase of the charge density of HA. Furthermore, the sulfation of HA may result in different sulfation patterns. In the case of low sHAs, this means that the sulfation is found exclusively at the primary hydroxyl groups, whereas for high sHAs, there is further sulfation at the secondary hydroxyl groups. Thus, the interaction with growth factors involved in bone homeostasis such as bone morphogenetic protein (BMP)-2, -4, and transforming growth factor-ß1 can be altered in a sulfation-dependent manner.[22−24] So, sHA derivatives can be used to mimic the naturally high-sulfated GAGs (heparin, heparan sulfate) in their role in the ECM to gain a deeper understanding of complex biological processes, which is required for GAG-controlled wound healing in bone tissue.

In previous studies, we showed positive effects of coll-based coatings containing high-sulfated HA on healing processes like the support of osteogenic differentiation of human mesenchymal stromal cells,[25] the support of osteoblast and osteocyte functions[26,27] as well as the inhibition of osteoclast differentiation and resorption.[11] Recent findings reveal that high-sulfated GAGs control osteoclastogenesis via interference with the osteoprotegerin (OPG) and receptor activator of NF-κB ligand (RANKL)/OPG complex formation and enhanced osteogenic potential by modulating sclerostin bioactivity.[28,29] Hence, sulfated HA derivatives are promising components for innovative biomimetic materials for the regulation of biological processes at the bone/biomaterial interface.

Replicating the biocomplexity of the native ECM is a goal that is critical for a detailed understanding of complex physiochemical and biochemical signals influencing cells during bone homestasis.[30] This knowledge will foster the design of functional biomaterials with defined bone-inducing properties for personalized medicine. In this study, low- and high-sulfated HA derivatives and coll type I are used to develop cellular microenvironments with increased complexity closer mimicking the biomolecular environment in vivo. Furthermore, the potential of sHA to fine-tune cellular responses with single-GAG matrices containing only one sHA derivative was studied by the systematic alteration of the GAG amount during in vitro fibrillogenesis. The purpose of this study was to engineer and fully characterize customized multi-GAG in comparison to single-GAG coatings and to reveal their modulatory potential on osteoclast-like cells. For this purpose a new combination of different analytical methods such as ζ-potential measurements and agarose gel electrophoresis of sHA derivatives was established.

2. EXPERIMENTAL SECTION

2.1. Materials. Native high molecular weight HA (from Streptococcus, MW (LLS) = 1.1 • 10^6 g/mol, PD = 4.8) was obtained from Aqua Biochem (Dessau, Germany), sulfur trioxide/dimethylformamide complex (SO_3-DMF, purum, ≥ 97%, active SO_3 ≥ 48%) and sulfur trioxide/pyridine complex (SO_3-pyridine, pract. ≥ 45% SO_3) from Fluka Chemie (Buchs, Switzerland). Rat coll type I was purchased from Corning (Kaiserslautern, Germany) and biochemical reagents were from Sigma-Aldrich (Schnelldorf, Germany). Fluorescence markers (ATTO 488-NH_2, ATTO 565-NH_2) were purchased from ATTO-TEC (Siegen, Germany).

2.2. Preparation of Modified HA Derivatives. The low- and high-sulfated HA derivatives (sHA1, sHA4) were synthesized and characterized as described previously.[22,31] Low molecular weight HA (LMW-HA) was prepared by ozonolysis of high molecular weight native HA. A 1% aqueous solution of high molecular weight HA was treated with ozone, prepared with an ozone generator COM-AD-02 (ANSEROS Klaus Nonnenmacher, Tübingen, Germany) for 2 h. The ozone concentration amounted to approximately 30 g O_3/m^3 and a flow rate of 20−30 l/h was used. Finally, N_2 was passed through the solution for 30 min to expel free ozone. The remaining clear, fluid solution was then dialyzed against distilled water, lyophilized, and dried in vacuum. The LMW-HA was obtained in 75−85% yield. Analytical data of the prepared HA derivatives (LMW-HA, sHA1, sHA4) are summarized in Table 1.

Table 1. Characteristic Parameters of HA Derivatives (degree of sulfation (D.S.), Number-Average (M_n) and Weight-Average (M_w) Molecular Weights As Revealed via Laser Light Scattering (LLS) Detection and Refraction (RI) Detection (in brackets), Molecular Weight Distributions (polydispersity index: PD) Calculated from RI Detection Values

sample	LMW-HA	sHA1	sHA4
D.S.		1.4	3.6
M_n (g/mol)	15 435 (40 105)	9625 (22 265)	19 25 (33 090)
M_w (g/mol)	23 040 (87 570)	20 255 (62 430)	28 610 (57 420)
PD	2.18	2.81	1.74

The functionalization of HA-derivatives (sHA1, sHA4) with fluorescence dyes (ATTO 565-NH_2 for sHA1, ATTO 488-NH_2 for sHA4) was carried out at the reducing end-groups of the macromolecules using the following general procedure: 0.4 mmol of sHA1 and sHA4, respectively, were dissolved in 30 mL of distilled water and the pH value was adjusted with 0.1 M NaOH to 8−8.5. Then, 500 μg of the fluorescence marker, dissolved in water (ATTO 488-NH_2) and DMSO (ATTO 565-NH_2), respectively, were added to the solution and the reaction mixture was stirred for 6 h at room temperature.

Coupling ATTO 565-NH_2 to sHA1, the pH of the mixture was then adjusted to 7.5 and 0.4 mmol $NaCNBH_3$ was added in two steps. After stirring for 3 days at room temperature, the reaction mixture was first dialyzed against water at pH 8−8.5 and afterward dialysis was continued against deionized water at pH 5.5 to remove residual unbound dye. In the case of coupling ATTO 488-NH_2 to sHA4, the reaction product was immediately dialyzed in the same manner as described. After filtration, lyophilization and drying in vacuum, the labeled polymers were obtained in ∼85% yield. The content of fluorescent labeling was estimated by measurement of the fluorescence

DOI: 10.1021/acsami.5b08419
ACS Appl. Mater. Interfaces 2015, 7, 23787−23797

intensity (TECAN reader infinite M1000 PRO) in relation to a standard curve obtained from pure fluorescent dye and subtraction of background fluorescence of unlabeled biopolymer. For the sHA1-ATTO 565 conjugate and the sHA4-ATTO 488 conjugate a content of fluorescence marker of 0.45 and 0.06 μg/mg, respectively, were found.

2.3. Preparation of Collagen-Based Coatings. Coll/GAG matrices were prepared as described by Hintze et al.[32] In brief, 1 mg/mL rat coll type I in ice-cold acetic acid (10 mM) was mixed in wells plates (Nunc, Langenselbold, Germany) with equivalent volumes of 1 mg/mL HA or the respective same molarity of disaccharides for all sHA derivatives dissolved in fibrillogenesis buffer (60 mM phosphate, pH 7.4) to prepare 1/1 matrices. The 1/0.5 coatings were produced by using 1:1 diluted solutions of sHA derivatives in fibrillogenesis buffer. For the preparation of the multi-GAG coating (1/0.5/0.5) equal volumes of the sHA1 and sHA4 solutions for the 1/1 coatings were mixed and used for fibrillogenesis with similar volumes of coll. Fibril formation via in vitro fibrillogenesis was initiated by rising the temperature to 37 °C. After 16−18 h of incubation at 37 °C, coatings were air-dried, washed twice with deionized water and dried again.

For cell culture experiments 24 well plates (Fisher Scientific, Schwerte, Germany) or glass slides were coated with matrices using the GAG derivatives without any fluorescence labels. PEEK foils (Invibio, Lancashire, United Kingdom) with a size of 1 × 2 cm were coated with matrices for ζ-potential measurements. Before use, the coatings for ζ-potential measurements and for cell culture experiments were incubated in PBS at 37 °C for 1 h.

2.4. Composition of Collagen-Based Coatings. The composition was studied after in vitro fibrillogenesis as well as after incubation in PBS at 37 °C for up to 8 days. The coll I amount in the coatings was calculated from the difference between the original amount used and the protein content in the supernatants determined by the method of Lowry et al. with coll I as the standard as described previously.[33,34] The 1,9-dimethylmethylene blue (DMMB) assay was used to determine the amount of sulfated GAGs bound to collagen after in vitro fibrillogenesis following papain incubation at 60 °C for 24 h.[32,35] HA content was determined by the hexosamine assay based on the Elson-Morgan reaction.[36] To distinguish sHA1 and sHA4 in the multi-GAG coating, we then prepared matrices with ATTO-labeled derivatives. The amount of fluorescent GAGs in the matrix was again determined after coll digestion with papain by fluorescence measurements (ATTO488: λ_{ex} = 488 nm, λ_{em} = 523 nm; ATTO565; λ_{ex} = 563 nm, λ_{em} = 592 nm). A corresponding solute GAG derivative treated similar was used for calibration.

2.5. Extraction and Separation of Sulfated HA Derivatives. The sHA derivatives were extracted from the dried coatings after papain digestion using a modified protocol from van de Lest et al.[37] In brief, to each matrix containing well of a 24 well plate 400 μL papain (0.1 mg/mL in PBS) was added. After digestion (24 h at 60 °C), peptides and proteins were removed by the addition of 100% (w/v) trichloroacetic acid to a final concentration of 6%. After 2 h on ice, the proteins and peptides were precipitated by centrifugation (30 min, 15000g, 4 °C). To the supernatant was added 4 vol of 100% ethanol and GAGs were allowed to precipitate for 16 h at −20 °C. After centrifugation (30 min, 15000g, 4 °C) GAGs were dried.

Agarose gel electrophoresis was used for sHA separation as described by Volpi et al. with some modifications.[38] Agarose gels (1%, 0.5 cm thick) were casted in 50 mM barium acetate (pH 5.0). GAG samples were dissolved in deionized water. Samples of 10 μL of a mixture of 10 μL HA sample and 3 μL sample application buffer (bromophenol blue) were applied to the gel. The gel run was performed in 50 mM barium acetate (pH 5.5) for 1 h at 60 V. After migration, the gels were incubated in a solution of 0.2% cetylpyridinium chloride. Afterward, the gels were stained with a 0.2% toluidine blue solution in ethanol/water/acetic acid (50/49/1, v/v/v) for 30 min and destained with a mixture of ethanol/water/acetic acid (50/49/1, v/v/v). The gels were further stained with Stains-all (25 mg in 500 mL 50% ethanol) overnight in the dark and destained with water and short exposure to light to reduce background. The gels were scanned with an Epson perfection 4180 photo scanner in the RGB mode. The corresponding GAGs served as control.

2.6. Morphology of Collagen-Based Coatings. The morphology of the resulting fibrils was examined via atomic force microscopy (AFM) as described previously.[34] In brief, coll/GAG fibrillogenesis solutions were prepared as described in 2.3. Fibrils formed after incubation at 37 °C were then subjected to centrifugation (15 min, 5000 g). Afterward, fibrils were reconstituted in 30 mM phosphate buffer (pH 7.4) via an ultrasound horn and adsorbed to mica substrates (Plano, Wetzlar, Germany). The surfaces were washed with deionized water and air-dried. Fibril morphology was assessed via AFM (Nanoscope IIIa Bioscope, Digital Instruments/Veeco, New York, USA) in tapping mode. Both height and amplitude images were acquired.

2.7. Surface ζ-Potential Measurements. The isoelectric points of GAG-containing coatings were measured by probing the dependence of the surface ζ-potential on pH as described by Altgärde et al.[39] The ζ-potential measurements of different coatings (coll, coll/HA (1/1), coll/sHA1/sHA4 (1/0.5/0.5), coll/sHA1 (1/1), coll/sHA4 (1/1)) were performed using the SurPASS instrument (Anton Paar, Graz, Austria) equipped with an adjustable gap cell. PEEK films were used as substrates for the deposition of the coatings and 0.1 M aqueous KCl as electrolyte. The pressure to generate the current was 400 mbar. To measure the ζ-potential in a range of pH-values between 2 and 10, the pH value was changed by the gradual addition of 0.05 M HCl or NaOH, respectively.

2.8. Cell Culture of Murine Osteoclast-Precursor-Like RAW264.7 Cells. To characterize the cellular effects of matrix compositions on bone residing cells, murine RAW264.7 cells were investigated as a model for osteoclasts. For expansion, RAW264.7 cells were cultivated in MEM-α (Biochrom) supplemented with 10% FCS (Biochrom), 1% penicillin/streptomycin (Gibco), 2 mM glutamine (Biochrom) up to 85% confluency before being passaged. For experiments, cells were detached with a cell scraper and seeded to matrix coated wells at a density of 12,500 cell/cm^2. Osteoclast differentiation was initiated by supplementation of the expansion medium with receptor activator of nuclear factor kappa-B ligand (RANKL, 20 ng/mL, R&D Systems, Wiesbaden-Nordenstadt, Germany).

2.9. Analysis of Osteoclast Differentiation. To investigate coating-induced effects at different stages of their differentiation, we measured viability as a marker of early coating induced effects, whereas changes in osteoclast number and morphology were detected to characterize long-term effects.

2.9.1. Osteoclast Precursor Viability. RAW264.7 cells were cultivated for 48 h in matrix-coated 48 or 24 well plates. Then, medium was changed to fresh medium supplemented with 10% CellTiterBlue reagent (CellTiterBlue, Promega, Mannheim, Germany) and incubated up to 2 h. Viability was then quantified by the conversion of the resazurin dye into a fluorescent product by metabolically active cells and measured using a FLUOStar Omega (λex = 560 nm/λem = 590 nm, BMG Labtech, Ortenberg, Germany).

2.9.2. Osteoclast Differentiation. Maturation status of osteoclasts was assessed after differentiating RAW264.7 cells on matrix coated multiwell plates for 5 days. Wells were then washed and stained for tartrate-resistant acid phosphatase (TRAP kit, Sigma-Aldrich, Schnelldorf, Germany). Finally, osteoclasts were quantified via the assessment of positively stained cells containing three or more nuclei.

2.9.3. Immunofluorescence. As a long-term marker, functional morphology was analyzed by staining RAW264.7 cells that were differentiated on glass slides coated with matrices as previously described.[11,40] In brief, upon the detection of mature osteoclast in the control wells after 72 h, cells were washed with PBS and fixed for 15 min with 4% paraformaldehyde. To allow for complete antigen accessibility, we permeabilized cells for 20 min in 0.1% Triton X-100/PBS followed by a brief washing and blocking step with 1% BSA, 0.05% Tween in PBS. Then, f-Actin and cell nuclei were visualized via Phalloidin-Alexa 488 (1:100) and DAPI staining (2.5 μg/mL, Life Technologies, Carlsbad, California, USA) and extensively washed afterward. To preserve fluorescence, we then embedded slides in

DOI: 10.1021/acsami.5b08419
ACS Appl. Mater. Interfaces 2015, 7, 23787−23797

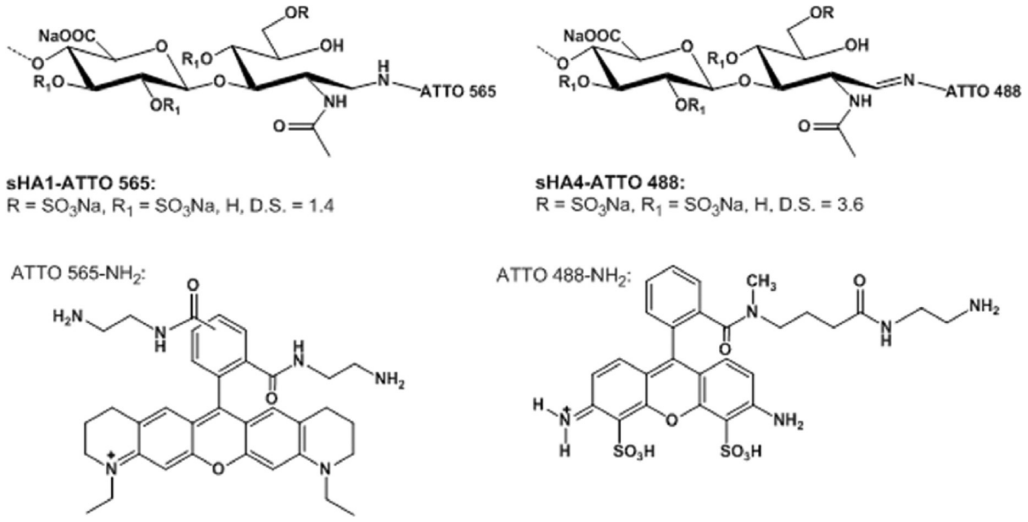

Figure 1. Fluorescence-labeled sHA derivatives.

mounting medium (Dako, Hamburg, Germany) before they were analyzed and documented via digital microscopy. For statistical analysis, images of at least 5 random spots of 3 slides were evaluated for the individual size and cumulative area covered by osteoclasts relative to a coll-coated control.

2.10. Statistics. For analysis of statistical significance, we repeated experiments at least in triplicates. Results represent mean ± standard deviation. One-way ANOVA or two-way ANOVA was applied. Bonferroni posthoc test was applied to evaluate differences between the groups. *P* values <0.05 were considered statistically significant.

3. RESULTS

3.1. Preparation of HA Derivatives. Low- and high-sulfated HA derivatives (sHA1, D.S. = 1.4; sHA4, D.S. = 3.6) with reduced molecular weight (MW (LLS) of 20 kDa, and 29 kDa, respectively) were synthesized and characterized as described previously.[22,31] As a nonsulfated reference material, a low molecular weight HA with a comparable molecular weight of MW (LLS) of 23 kDa was derived by ozonolysis of native HA with high molecular weight. ^{13}C NMR investigations of this degraded HA do not show any structural changes compared to native HA (data not shown).

The functionalization of HA sulfates (sHA1, sHA4) with amino group containing fluorescence markers (ATTO 565-NH2, ATTO 488-NH_2) was carried out at the reducing end-groups of the HA molecules. We tried to reduce the newly formed imine structure with a C═N double bond with sodium cyanoborohydride ($NaCNBH_3$) to form the more stable amine. However, the sHA4-ATTO 488-conjugate lost its fluorescence activity after treatment with $NaCNBH_3$ and was therefore used in the nonreduced imine form. The structures of the fluorescence-labeled GAGs are shown in Figure 1.

3.2. Composition and Stability of Collagen-Based Coatings. The coating composition and stability were studied after in vitro fibrillogenesis as well as after incubation in PBS at 37 °C for up to 8 days. After washing all coatings contained 10−15% of the original GAG amount used (Figure 2 A). The highest GAG release occurs during the first hour of matrix incubation, while at later time points the release is only marginal. The percentage of remaining GAG per coating is significantly higher for the 1/0.5 matrix than for the 1/1 aECM with sHA4, whereas there are no differences between the 1/1 and 1/0.5 matrices for the other applied GAGs. In general, the

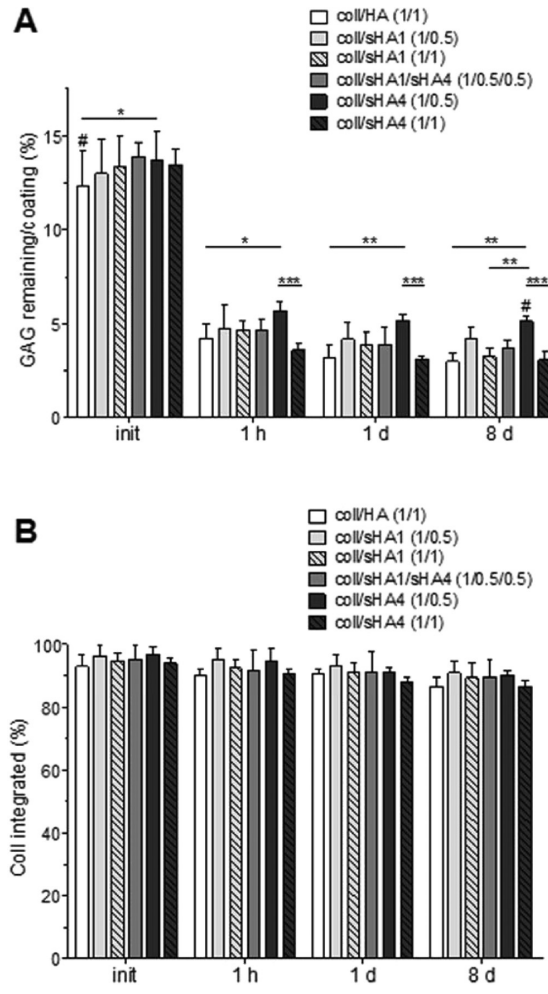

Figure 2. Composition of coatings. Matrices were washed twice with deionized water (init) and incubated in PBS for up to 8 days at 37 °C. The GAG content (A) was examined by DMMB and hexosamine (Elson-Morgan reaction) assays; the collagen I content (B) was determined by Lowry method. Two-way ANOVA: **p* < 0.05; ***p* < 0.01; ****p* < 0.001 vs respective coating; #*p* < 0.05; ##*p* < 0.01 vs the multi-GAG matrix only.

DOI: 10.1021/acsami.5b08419
ACS Appl. Mater. Interfaces 2015, 7, 23787−23797

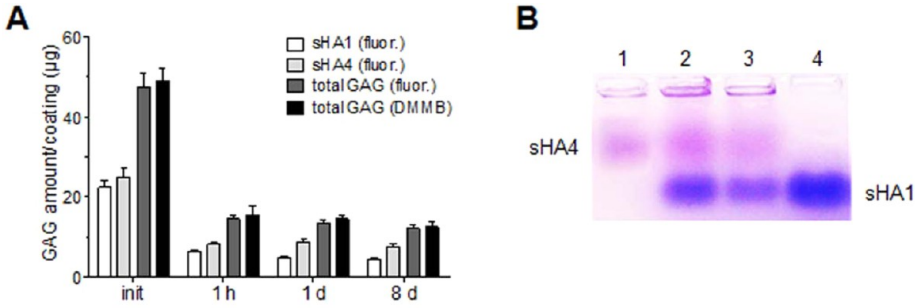

Figure 3. Quantification and visualization of sHA contents of the multi-GAG coating. (A) sHA content in the multi-GAG coating (init = GAG content after two washing steps with deionized water) assessed by fluorescence measurements and DMMB assay. (B) GAGs isolated from the multi-GAG coating, separated by agarose gel electrophoresis in 50 mM barium acetate (pH 5.0) and stained by toluidine blue and Stains-all. Lane 1, sHA1 reference (10 μg); lane 2, sHA derivatives isolated from the matrix after washing with deionized water; lane 3, sHA derivatives isolated from the matrix after 1 h desorption in PBS; lane 4, sHA4 reference (10 μg).

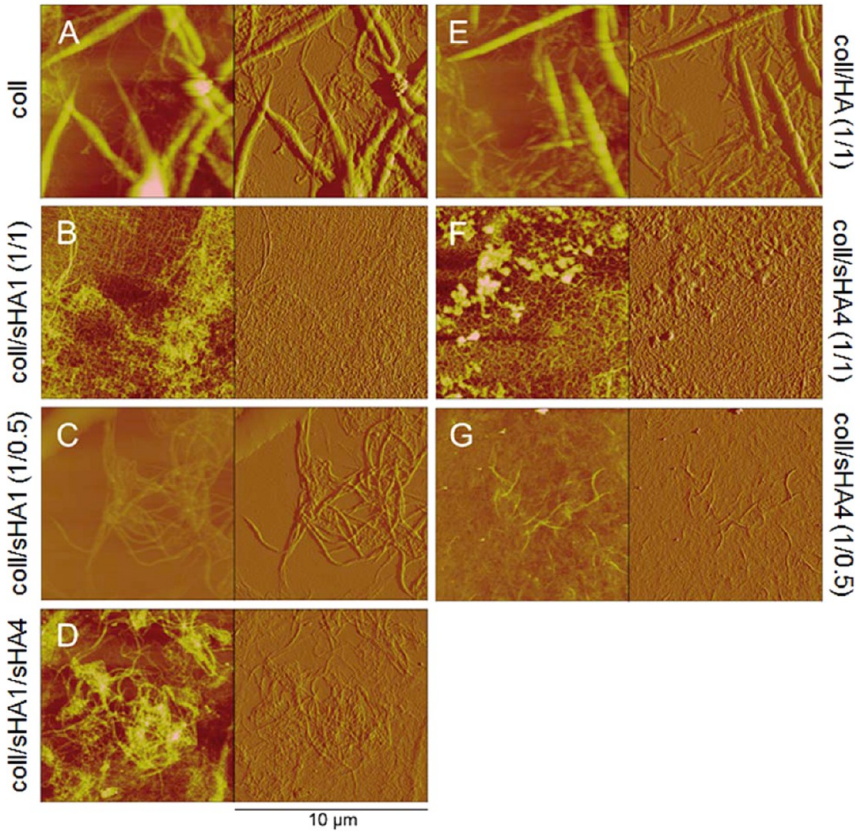

Figure 4. Matrix topography in the presence of HA and sHA. Collagen fibrillogenesis was performed at 37 °C in the absence or presence of different GAGs examined by AFM. (A) coll without GAGs; (B) coll/sHA1 (1/1); (C) coll/sHA1 (1/0.5); (D) coll/sHA1/sHA4 (1/0.5/0.5); (E) coll/HA (1/1); (F) coll/sHA4 (1/1); and (G) coll/sHA4 (1/0.5). The panels show 10 × 10 μm sections as height images (left column) and amplitude images (right column).

percentage of integrated GAGs relative to the initial GAG amount present during fibrillogenesis of the multi-GAG matrices were comparable with those of the 1/1 single-GAG coatings with HA, sHA1 or sHA4.

About 90−95% of the applied coll monomers (200 μg each) are integrated into the aECMs regardless of the GAG derivative or the GAG amount applied during fibrillogenesis and the content remains quite stable over time (Figure 2B). There are no significant differences of the coll content between the GAG-containing matrices (Figure 2B) as well as the coll reference (data not shown). After 1 h of incubation in PBS, the generated coatings exhibit coll and GAG mass ratios of 19:1 for coll/HA (1/1), 27:1 for coll/sHA1 (1/0.5), 13:1 for coll/sHA1 (1/1), 11:1 for coll/sHA1/sHA4 (1/0.5/0.5), 12:1 for coll/sHA4 (1/1), and 16:1 for coll/sHA4 (1/0.5) respectively.

Fluorescence-labeled derivatives of sHA1 and sHA4 were used to quantify the amount of each GAG in the multi-GAG coating and DMMB assay was performed to determine the total amount of sulfated GAGs. Similar results were obtained for the fluorescence measurement and the DMMB assay (Figure 3A). To verify these finding, we prepared multi-GAG coatings with unlabeled GAGs and examined the remaining GAGs after extraction from the coatings. Agarose gel electrophoresis analysis in barium acetate was used to separate sHA1 and

DOI: 10.1021/acsami.5b08419
ACS Appl. Mater. Interfaces 2015, 7, 23787−23797

sHA4 by their degree of sulfation due to ion pair formation between the sulfate groups of the GAGs and the barium ions which leads to a decreased electrophoretic mobility of the polysaccharides in the gel. Figure 3B illustrates the separation of sHA1 and sHA4. After treatment with toluidine blue and Stains-all, sHA1 appeared as a strong blue band while sHA4 appeared as purple band due to the metachromasia typical for sulfated polysaccharides.[41] A good resolution between these GAGs was achieved, with sHA1 and sHA4 having a mobility of 5.1 and 3.7 cm/(A h) at an electric field strength of 451 V/m, respectively. Qualitative analysis of the isolated HA derivatives compared to sHA standards reveals that both sHA derivatives (sHA1 and sHA4) are part of the multi-GAG coating (Figure 3B).

3.3. Topography of Collagen-Based Coatings. The structure of coll fibrils formed in the presence of HA as well as sHA derivatives was revealed by AFM (Figure 4). When HA was added prior to fibrillogenesis, the matrix morphology was comparable to coll in the absence of GAGs with an apparent banding pattern (Figure 4A, E).

The presence of sHA4 during in vitro fibrillogenesis results in microfibrils appearing like a homogeneous network but without a visible banding pattern (Figure 4F, G). Increasing the sHA1 concentration from 1/0.5 to 1/1 however causes significant changes in fibril morphology (Figure 4B, C). With increasing concentrations of sHA1 the fibril diameter decreases. For the 1/1 coll/sHA1 matrix only few microfibrils are visible embedded in network-like structures. The multi-GAG coating is heterogeneous, consisting of thin fibrils and microfibrils (Figure 4D).

3.4. Surface Charge of Collagen-Based Coatings. Because of the anionic nature of HA and especially of sHA derivatives, we expect a significant change in the surface charge of the matrices when GAGs are associated with the forming coll fibrils. The isoelectric points (pI) of coatings were determined by probing the dependence of the surface ζ-potential on pH values.

The resulting curves for the 1/1 GAG-containing coatings as well as the multi-GAG matrices are shown in Figure 5. The coll reference displayed an isoelectric point close to 6.5, which is in the range between 5.3−7.5 reported in the literature.[42] The GAG-containing coatings, however, revealed lower pI values. With increasing degree of sulfation, the isoelectric point of the coatings decreased. The isoelectric point of the multi-GAG matrix was in-between the 1/1 matrices containing sHA1 or sHA4 alone.

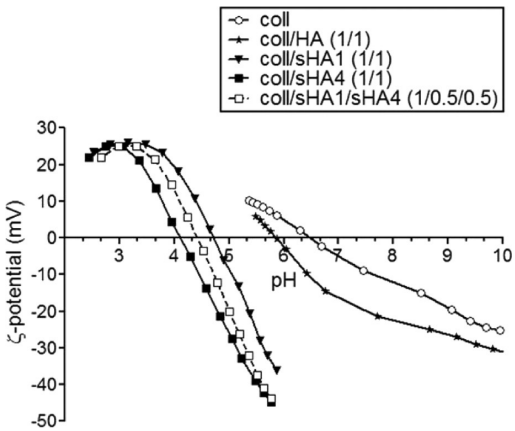

Figure 5. Influence of HA and sHA on the ζ-potential of coll-based coatings. ζ-potential as a function of the pH for coatings with or without HA or sHA. A matrix of coll is included as a reference.

3.5. Effects of Different GAG Compositions on Osteoclastogenesis. Forty-eight hours after seeding, viability of differentiating RAW264.7 cells was determined to analyze the toxicity of coatings on osteoclast precursor cells. According to our previous study on the impact of GAG sulfation on osteoclast differentiation,[11] viability was significantly upregulated when grown on matrices containing sulfated GAGs (Figure 6A, coll/sHA). However, cells cultured on coatings with LMW-HA did not yield the significant down regulation observed for the native high-molecular-weight HA used in the previous study (Figure 6A, coll/HA). In single-GAG coatings there was no dose-dependent effect on cell viability. Although the sulfate content of the multi-GAG coating was lower compared to the single-component sHA4 matrices, viability of cells grown on the multi-GAG matrix was comparable (Figure 6A, coll/sHA4 vs coll/sHA1/sHA4).

Corresponding results were obtained when osteoclast precursors were analyzed after 4 days in culture. The LMW-HA derivative did not alter osteoclast number, whereas in general increasing sulfate content of the coatings reduced osteoclast formation (Figure 6B). Although TRAP-positive cells could be observed on the coatings with the sulfated GAGs only a minority of these contained three or more nuclei resulting in a diminished intensity of the TRAP-staining (Figure 6C). The osteoclast differentiation is suppressed in the following order: coll/sHA4 > coll/sHA1/sHA4 > coll/sHA1, or coll/HA > coll. This suppression is not only sulfation but in case of sHA4-containing coatings also dose-dependent. Interestingly, when cultured on the multi-GAG coating, the number of osteoclasts was higher than on coll/sHA4 (1/0.5) even though the overall sulfate content was higher as well (see section 3.2).

3.6. Impact of Sulfate Modification of GAGs on Functional Morphology. To better reflect this finding, we seeded osteoclast precursor cells on differently coated glass slides, stained to visualize their cytoskeleton and examined for changes in osteoclast functional morphology. Whereas large, multinucleated osteoclasts containing the characteristic actin belt were found on coll alone after 4 days (data not shown), cells cultured on coatings comprising HA tended to be smaller. However, these cells formed similar podosomal structures with no changes on osteoclast sealing zone morphology (Figure 7A, E).

As described before,[11] sulfate-modified GAGs in the matrices reduced osteoclast maturation leading to only small osteoclasts with few nuclei. Also, these osteoclasts were devoid of the characteristic sealing zonelike structures and instead displayed dendritic like appendages at the cell periphery (Figure 7C, D). Although quite abundant, the area covered by these premature osteoclasts was 7 times smaller (Figure 7E). When quantified, this smaller area could be ascribed to a reduced single cell size, whereas osteoclasts cultured on HA containing coatings were at average twice as large (Figure 7F) as osteoclasts formed on high-sulfated GAG derivatives.

4. DISCUSSION

The aim of our present study was to develop and to biochemically characterize a coll type I-based multi-GAG coating containing hyaluronan derivatives with different degrees of sulfation. In particular the goal was to evaluate the regenerative potential of this matrix in comparison to single-

DOI: 10.1021/acsami.5b08419
ACS Appl. Mater. Interfaces 2015, 7, 23787−23797

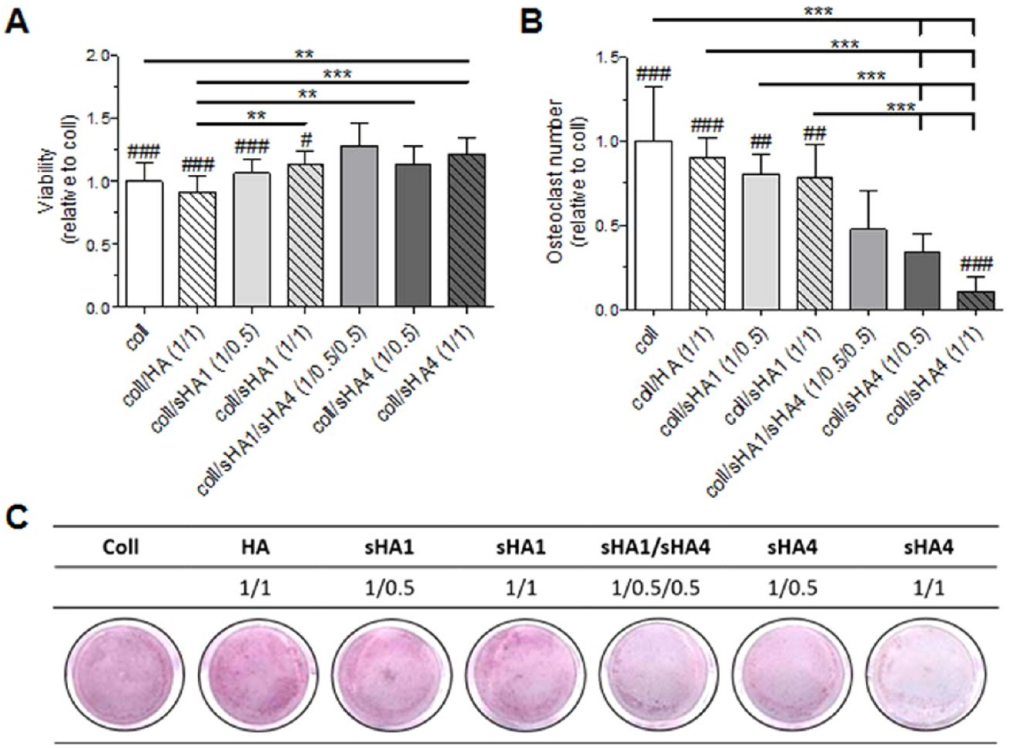

Figure 6. Influence of HA and sHA3 on osteoclast precursor viability and maturation. (A) Viability of RAW264.7 cells was analyzed after 48 h by resazurin conversion. (B) Osteoclast formation was measured by quantification of multinucleated (≥3), TRAP-positive cells. (C) Representative overview of TRAP stained wells after cell cultivation on different coatings. $^{**}p < 0.01$, $^{***}p < 0.001$ vs respective treatment; $\#p < 0.05$, $\#\#\#p < 0.001$ one-way ANOVA vs coll/sHA1/sHA4 (1/0.5/0.5).

GAG matrices with altered GAG amounts for improving bone remodeling by influencing the viability and osteoclastogenesis of osteoclast-precursor like cells.

Coll matrices containing two HA derivatives with different degrees of sulfation and single-GAG coatings with systematically altered GAG amounts were produced via in vitro fibrillogenesis of coll in the presence of GAGs without further cross-linking of these coatings, facilitating a release of GAGs and coll degradation over time. Together, these coatings provide an interesting model to design and study ECM mimicking biomaterials for tissue engineering applications since the GAG concentrations in these matrices were in the same range as in bone ECM with 4−5% of the coll dry weight sGAGs.[34,43]

One challenge of characterizing multi-GAG coatings is the simultaneous detection and quantification of two sulfated GAGs with a similar carbohydrate backbone in the low microgram range. For chemically modified HA derivatives no antibodies are available and due to the fact that the degradation via hyaluronidases is insufficient no fragment based discrimination is possible.[44] Also the standard assays for sulfated GAGs are not able to discriminate between these GAGs.[35,36] To quantify the amount of low- and high-sulfated HA within one matrix, fluorescent derivatives of sHA1 and sHA4 with different fluorescent dyes linked to the reducing end of GAGs were synthesized. In addition, different biochemical assays for GAG quantification were combined with agarose gel electrophoresis to allow discriminating between different sHA derivatives and therefore in-depth analysis of coating composition. The latter was used for the first time to separate sHA derivatives.

The coll amount for the preparation of the coatings was kept constant by varying the sulfation degree, the number and concentration of GAGs. In general, the amount of GAG associated coll increases with increasing the GAG concentration during in vitro fibrillogenesis. This finding is in line with previous studies.[34,45−47] However, there is no direct correlation of the amount of applied and integrated GAG as already shown by Miron et al. and Bierbaum et al.[34,45] The determined mass ratio of coll and LMW-HA in the present study are similar to those reported previously, whereas the content of sHA4 was higher.[48] The latter might be attributed to differences in sulfation degree and molecular weight. Fluorescence measurements as well as agarose gel electrophoresis reveal that both sHA-derivatives were integrated into the multi-GAG matrix and present even after different incubation times in PBS at 37 °C.

As native GAGs like heparin, HA and CS are known to organize other ECM components like the coll fibril formation (reviewed in[34]), one hypothesis was that GAGs individually alter the coll morphology of matrices. The AFM images of the coatings show a decrease in fibril diameter with increased GAG concentration and sulfation degree as already shown for coll type II[32] and coll type I[34] in the presence of single GAGs. The presence of two sHA derivatives with different degree of sulfation leads to a mixture of microfibrils and thin fibrils. This result suggests, that the fibril formation of coll is affected by both GAGs present leading to thin fibrils like in the presence of the low-sulfated HA derivative alone and microfibrils like in the presence of higher charged sHA4. Interestingly, these findings reveal that the morphology of the resulting matrix can be controlled by altering the self-assembly process of coll type I in a GAG- and sulfation-dependent manner. As coll and GAGs binding is largely of electrostatic nature,[49−52] the GAG's negative charge has shown to exhibit a far stronger impact on the fibril formation and thereby fibril topography than simply

DOI: 10.1021/acsami.5b08419
ACS Appl. Mater. Interfaces 2015, 7, 23787−23797

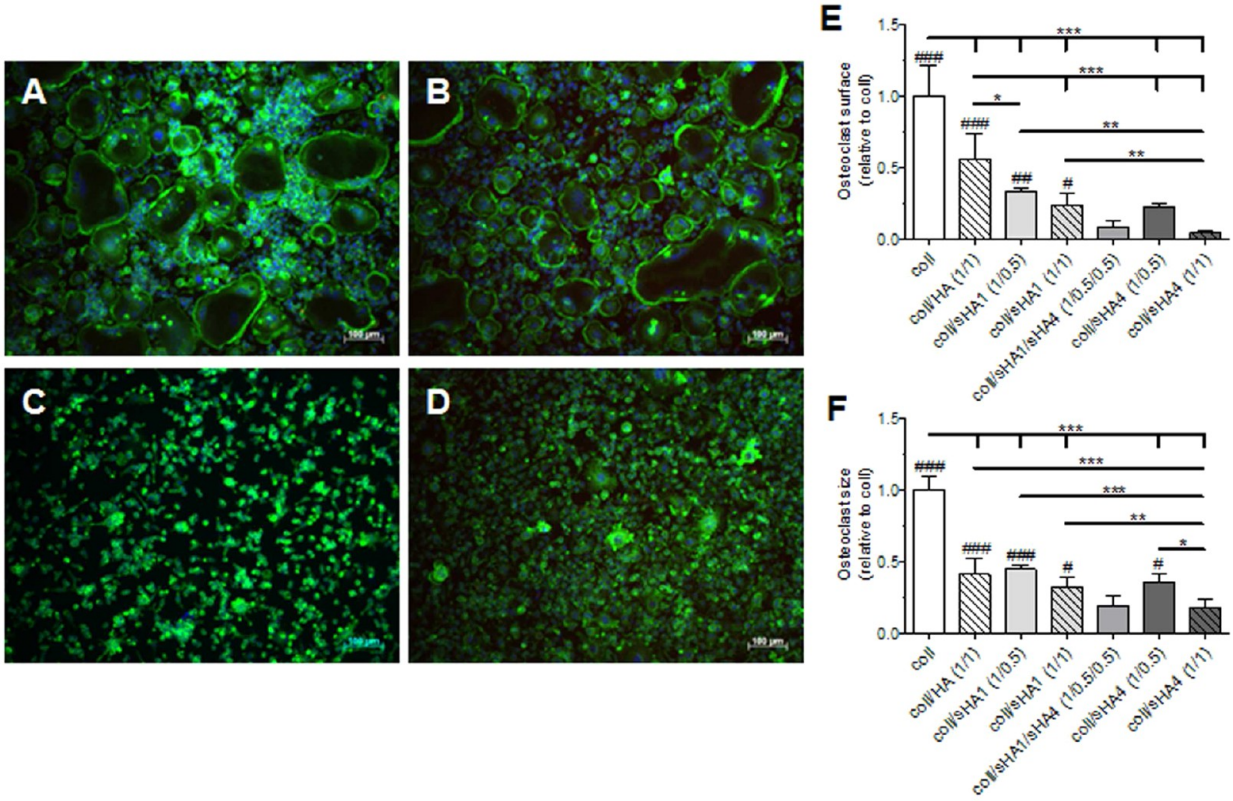

Figure 7. Influence of HA and sHA on differentiation and functional morphology of RAW264.7 cells. Monocytic RAW264.7 cells were differentiated for 4 days. Osteoclast differentiation was then examined after immunofluorescence staining of f-actin (green, phalloidin-AlexaFluor 488) and cell nuclei (blue, DAPI). A-D: Representative pictures of A: coll/HA, B: coll/sHA1 (1/1), C: coll/sHA4 (1/1) and D: coll/sHA1/sHA4 (1/0.5/0.5). E-F: Quantitative analysis via ImageJ of E: osteoclast surface and F: osteoclast size. *$p < 0.05$, **$p < 0.01$, ***$p < 0.001$ vs respective treatment; #$p < 0.05$, ##$p < 0.01$, ###$p < 0.001$ one-way ANOVA vs coll/sHA1/sHA4 (1/0.5/0.5).

increasing GAG concentrations,[51] as apparent for increased sHA4 concentrations in comparison to the sHA1 or HA containing coatings.

To study the influence of GAGs associated with coll on the surface charge the ζ-potential of the coatings was examined. The matrix with coll alone displayed the highest isoelectric point of the examined coatings (~6.5). Freudenberg et al., reported a dependence of the pI of coll type I on the ionic strength in KCl solution (pH 7.5−5.3). For a comparable ionic strength they determined a pI of 5.3.[42] This difference might be due to varying collagen sources and formulations. The combination of GAGs with coll should lead to decreased pI values compared to coll alone due to the anionic nature of GAGs. As expected, the isoelectric point of the coatings was sulfation-dependently reduced in the following order: coll/sHA4 < coll/sHA1/sHA4 < coll/sHA1 < coll/HA < coll. These findings highlight the prospect of multi-GAG coatings to adjust defined surface charge properties. For HA alone the expected pI is ~2.5,[53] whereas for sHA derivatives, because of the anionic sulfate groups, values are expected to be even lower. However, Altgärde et al. determined pI values in the range of 3.5 and 4 for sHA and HA.[39] For GAG-containing coatings the pI values were higher than for GAGs alone since some of the anionic charge of the GAGs is compensated by the association of the negatively charged groups (carboxyl and sulfate groups) with positively charged regions of the collagen fibrils. A further explanation is a lower surface density of GAGs in coatings compared to measurements with GAGs alone.

The intercellular communication between osteoblasts and osteoclasts is an integral element in bone homeostasis as demonstrated by many metabolic bone diseases which are associated with a disrupted cross-talk between these cells.[54] In this study, we used LMW-HA (23 kDa) produced by ozonolysis in comparison to sHA derivatives with molecular weights in the same range to compare the influence of GAG sulfation on cell function. In contrast to previous finding with matrices containing native HA (molecular weight of about 1000 kDa),[11] the LMW-HA did not significantly change the viability of RAW264.7 cells. Our results are in line with reports from Lee et al. for LMW-HA (50 kDa)[55] and maybe due to the different chain length of native HA compared to LMW-HA. Interestingly, Ariyoshi et al. reported an enhanced osteoclast formation in the presence of LMW-HA (<8 kDa), whereas HA with a molecular weight higher than 90 kDa showed no effects.[56] Our results revealed no influence of LMW-HA (23 kDa) on osteoclastogenesis which can be explained by the differences in the molecular weight.

No dose-dependent effects on cell viability were detectable for the single-GAG matrices. Surprisingly, we observed a significant increase in cell viability on the coating containing both sHA1 and sHA4 alike those containing sHA4 compared to the other matrices. This indicates a synergistic effect of sGAGs within the multi-GAG coating. However, at the same time the number of differentiated osteoclasts was higher than on coll/sHA4 (1/0.5) despite a higher sulfate content. These data indicate that the impact of these coatings on osteoclastogenesis is not only determined by the sulfation degree and the overall

DOI: 10.1021/acsami.5b08419
ACS Appl. Mater. Interfaces 2015, 7, 23787−23797

amount of charge present. Furthermore, these results suggest that the multi-GAG composition of coatings allows for discrete fine-tuning of GAG effects on tissue residing cells that might rescue the intimate communication between osteoclasts and osteoblasts. This is quite important for the long-term stability of bone implants.

The different matrix morphologies and surface charges may also influence the observed effects for example by altering the interaction profile of the coll fibrils formed in the present of GAGs to cell surface receptors like integrins. However, we suggest that differences in the morphology are of secondary importance in this study, because solute GAGs exert comparable results on osteoclast differentiation.[26]

The mechanisms of GAG-controlled osteoclastogenesis are not completely understood today. One possible mechanism is the direct influence of GAG sulfation on receptor−ligand communication. Ariyoshi et al. recently reported that the interaction of high-molecular weight HA with the HA receptor CD44 is able to down-regulate RANKL expression and osteoclastogenesis via activation of the Rho kinase pathway.[57] A second mechanism could be the influence of sGAGs on cell adhesion and spreading. For example, heparin was already shown to strongly decrease the adherence of osteoclast precursors and to inhibit spreading and activity of osteoclasts.[58] Another important aspect is the modulation of signaling cascades crucial for osteoclastogenesis by sGAGs. In line with our findings, previous studies revealed that the presence of high-sulfated GAGs like heparin suppress the formation of TRAP-positive multinucleated cells and inhibit the formation of resorption pits. One possible explanation is that RANKL binds to sGAGs and these GAG/RANKL complexes are not able to induce osteoclastogenesis.[59] In contrast to this Salbach-Hirsch et al. reported that sGAGs bind to OPG but not to RANKL in a sulfation-dependent manner, controlling osteoclastogenesis by interference with the RANKL/OPG complex formation.[28] Beside these explanations, the interaction of GAGs with a variety of further mediator proteins involved in bone homeostasis and regulation such as members of the transforming growth factor-β superfamily like BMP-2 and -4 needs to be considered.[22,23]

We recognize potential limitations of our study such as a limited number and concentrations of GAG derivatives, and a rather uniform backbone structure missing iduronic acid present in heparan sulfate/heparin. Future work will include GAG derivatives with different sulfation patterns to investigate the impact of GAG concentration and sulfate distribution within the polymer on cell activity. Further alterations of the sugar backbone will improve the control of direct and indirect cellular interactions with the matrices.

Taken together, this study illustrates the application of bioinspired cellular microenvironments as cell-instructive implant coatings with focus on developing coll-based matrices with two distinct HA derivatives as well as matrices with different GAG concentrations and sulfation able to engineer signals of the native ECM into biomaterials. The incorporation of two sHA derivatives with different sulfation degrees and pattern into the coatings was shown to provide a favorable environment for osteoclast precursor-like cells. These findings highlight the importance of developing biomaterials replicating the biocomplexity of the native ECM to provide a deeper understanding of complex physiochemical and biochemical factors like GAG sulfation and concentration as well as the interplay of differently sulfated GAGs on cell functions. Thus, multi-GAG coatings, which are inspired by the coll-GAG assemblies in native ECMs, can be favorable as customized implant coating for controlling healing processes in bone.

5. CONCLUSION

GAG-containing coatings with defined physiological effects can be developed by varying their GAG content and composition. The analysis of multi-sHA in comparison to single-sHA matrices revealed that osteoclast-precursor survival and osteoclastogenesis is influenced by the interplay of different GAG derivatives, which is not only a simple effect of the sulfation degree or the overall amount of charge. These insights allow for the precise adjustment of bone cell responses. Thus, in particular, coatings composed of coll and multiple sHAs are promising candidates that might hold the potential to advance functional biomaterials and coatings toward patient-specific needs.

AUTHOR INFORMATION

Corresponding Author

*E-mail: Dieter.Scharnweber@tu-dresden.de.

Notes

The authors declare no competing financial interest.

ACKNOWLEDGMENTS

We acknowledge financial support by the German research foundation Transregio 67 [subprojects A2, A3, B2, Z3].

ABBREVIATIONS

AFM, atomic force microscopy; BMP, bone morphogenetic protein; coll, collagen; CS, chondroitin sulfate; D.S., degree of sulfation; ECM, extracellular matrix; GAG, glycosaminoglycan; HA, hyaluronan; LLS, laser light scattering; LMW, low molecular weight; Mn, number-average molecular weigth; Mw, weight-average molecular weight; OPG, osteoprotegerin; PD, polydispersity index; pI, isoelectric point; RANKL, receptor activator of NF-κB ligand; RI, refraction detection; sHA, sulfated hyaluronan; TRAP, tartrate-resistant acid-phosphatase

REFERENCES

(1) Brydone, A. S.; Meek, D.; Maclaine, S. Bone Grafting, Orthopaedic Biomaterials, and the Clinical Need for Bone Engineering. *Proc. Inst. Mech. Eng., Part H* **2010**, *224* (12), 1329−1343.

(2) Hernandez, R. K.; Do, T. P.; Critchlow, C. W.; Dent, R. E.; Jick, S. S. Patient-related Risk Factors for Fracture-healing Complications in the United Kingdom General Practice Research Database. *Acta Orthop.* **2012**, *83* (6), 653−660.

(3) Hidalgo-Bastida, L. A.; Cartmell, S. H. Mesenchymal Stem Cells, Osteoblasts and Extracellular Matrix Proteins: Enhancing Cell Adhesion and Differentiation for Bone Tissue Engineering. *Tissue Eng., Part B* **2010**, *16* (4), 405−412.

(4) Badylak, S. F.; Freytes, D. O.; Gilbert, T. W. Extracellular Matrix as a Biological Scaffold Material: Structure and Function. *Acta Biomater.* **2009**, *5* (1), 1−13.

(5) Di Lullo, G. A.; Sweeney, S. M.; Körkkö, J.; Ala-Kokko, L.; San Antonio, J. D. Mapping the Ligand-Binding Sites and Disease-associated Mutations on the Most Abundant Protein in the Human, Type I Collagen. *J. Biol. Chem.* **2002**, *277* (6), 4223−4231.

(6) Robey, P. G.; Boskey, A. L. The Composition of Bone. *Bone Miner.* **2008**, 32−38.

(7) Sasisekharan, R.; Raman, R.; Prabhakar, V. Glycomics Approach to Structure-function Relationships of Glycosaminoglycans. *Annu. Rev. Biomed. Eng.* **2006**, *8*, 181−231.

DOI: 10.1021/acsami.5b08419
ACS Appl. Mater. Interfaces 2015, 7, 23787−23797

(8) Imberty, A.; Lortat-Jacob, H.; Perez, S. Structural View of Glycosaminoglycan-protein Interactions. *Carbohydr. Res.* **2007**, *342* (3−4), 430−439.
(9) Mania, V. M.; Kallivokas, A. G.; Malavaki, C.; Asimakopoulou, A. P.; Kanakis, J.; Theocharis, A. D.; Klironomos, G.; Gatzounis, G.; Mouzaki, A.; Panagiotopoulos, E.; Karamanos, N. K. A Comparative Biochemical Analysis of Glycosaminoglycans and Proteoglycans in Human Orthotopic and Heterotopic Bone. *IUBMB Life* **2009**, *61* (4), 447−452.
(10) Rai, B.; Nurcombe, V.; Cool, S. M. Heparan Sulfate-based Treatments for Regenerative Medicine. *Crit. Rev. Eukaryotic Gene Expression* **2011**, *21* (1), 1−12.
(11) Salbach, J.; Kliemt, S.; Rauner, M.; Rachner, T. D.; Goettsch, C.; Kalkhof, S.; von Bergen, M.; Möller, S.; Schnabelrauch, M.; Hintze, V.; Scharnweber, D.; Hofbauer, L. C. The effect of the degree of sulfation of glycosaminoglycans on osteoclast function and signaling pathways. *Biomaterials* **2012**, *33* (33), 8418−8429.
(12) Prince, C. W.; Navia, J. M. Glycosaminoglycan Alterations in Rat Bone Due to Growth and Fluorosis. *J. Nutr.* **1983**, *113* (8), 1576−1582.
(13) Schulz Torres, D. S.; Freyman, T. M.; Yannas, I. V.; Spector, M. Tendon Cell Contraction of Collagen-GAG Matrices In Vitro: Effect of Cross-linking. *Biomaterials* **2000**, *21*, 1607−1619.
(14) Yannas, I. V.; Lee, E.; Orgill, D. P.; Skrabut, E. M.; Murphy, G. F. Synthesis and Characterization of a Model Extracellular Matrix that Induces Partial regeneration of Adult Mammalian Skin. *Proc. Natl. Acad. Sci. U. S. A.* **1989**, *86* (3), 933−937.
(15) Chamberlain, L. J.; Yannas, I. V.; Hsu, H. P.; Strichartz, G. R.; Spector, M. Near-terminus Axonal Structure and Function Following Rat Sciatic Nerve Regeneration Through a Collagen-GAG Matrix in a Ten-millimeter Gap. *J. Neurosci. Res.* **2000**, *60* (5), 666−677.
(16) Lin, J. T.; Lane, J. M. Osteoporosis. *Clin. Orthop. Relat. Res.* **2004**, *425* (425), 126−134.
(17) Spector, M. An interview with I V Yannas. Tracing One of the Deepest Roots of Biomaterials in Tissue Engineering/Regenerative Medicine. *Biomed. Mater.* **2013**, *8* (4), 040401.
(18) Hortensius, R. A.; Harley, B. A. C. The Use of Bioinspired Alterations in the Glycosaminoglycan Content of Collagen-GAG Scaffolds to Regulate Cell Activity. *Biomaterials* **2013**, *34* (31), 7645−7652.
(19) Kirker, K. R.; Luo, Y.; Nielson, J. H.; Shelby, J.; Prestwich, G. D. Glycosaminoglycan Hydrogel Films as Bio-interactive Dressings for Wound Healing. *Biomaterials* **2002**, *23* (17), 3661−3671.
(20) Allison, D. D.; Grande-Allen, K. J. Review. Hyaluronan: a Powerful Tissue Engineering Tool. *Tissue Eng.* **2006**, *12* (8), 2131−2140.
(21) Schiller, J.; Becher, J.; Möller, S.; Nimptsch, K.; Riemer, T.; Schnabelrauch, M. Synthesis and Characterization of Chemically Modified Hyaluronan and Chondroitin Sulfate. *Mini-Rev. Org. Chem.* **2010**, *7* (4), 290−299.
(22) Hintze, V.; Moeller, S.; Schnabelrauch, M.; Bierbaum, S.; Viola, M.; Worch, H.; Scharnweber, D. Modifications of Hyaluronan Influence the Interaction with Human Bone Morphogenetic Protein-4 (hBMP-4). *Biomacromolecules* **2009**, *10* (12), 3290−3297.
(23) Hintze, V.; Samsonov, S. A.; Anselmi, M.; Moeller, S.; Becher, J.; Schnabelrauch, M.; Scharnweber, D.; Pisabarro, M. T. Sulfated Glycosaminoglycans Exploit the Conformational Plasticity of Bone Morphogenetic Protein-2 (BMP-2) and Alter the Interaction Profile with its Receptor. *Biomacromolecules* **2014**, *15* (8), 3083−3092.
(24) Hintze, V.; Miron, A.; Moeller, S.; Schnabelrauch, M.; Wiesmann, H.-P.; Worch, H.; Scharnweber, D. Sulfated Hyaluronan and Chondroitin Sulfate Derivatives Interact Differently with Human Transforming Growth Factor-β1 (TGF-β1). *Acta Biomater.* **2012**, *8* (6), 2144−2152.
(25) Hempel, U.; Hintze, V.; Möller, S.; Schnabelrauch, M.; Scharnweber, D.; Dieter, P. Artificial Extracellular Matrices Composed of Collagen I and Sulfated Hyaluronan with Adsorbed Transforming Growth Factor β1 Promote Collagen Synthesis of Human Mesenchymal Stromal Cells. *Acta Biomater.* **2012**, *8* (2), 659−666.
(26) Salbach-Hirsch, J.; Ziegler, N.; Thiele, S.; Moeller, S.; Schnabelrauch, M.; Hintze, V.; Scharnweber, D.; Rauner, M.; Hofbauer, L. C. Sulfated Glycosaminoglycans Support Osteoblast Functions and Concurrently Suppress Osteoclasts. *J. Cell. Biochem.* **2014**, *115* (6), 1101−1111.
(27) Tsourdi, E.; Salbach-Hirsch, J.; Rauner, M.; Rachner, T. D.; Moeller, S.; Schnabelrauch, M.; Scharnweber, D.; Hofbauer, L. C. Glycosaminoglycans and their Sulfate Derivatives Differentially Regulate the Viability and Gene Expression of Osteocyte-like Cell Lines. *J. Bioact. Compat. Polym.* **2014**, *29* (5), 474−485.
(28) Salbach-Hirsch, J.; Kraemer, J.; Rauner, M.; Samsonov, S. A.; Pisabarro, M. T.; Moeller, S.; Schnabelrauch, M.; Scharnweber, D.; Hofbauer, L. C.; Hintze, V. The Promotion of Osteoclastogenesis by Sulfated Hyaluronan through Interference with Osteoprotegerin and Receptor Activator of NF-κB Ligand/Osteoprotegerin Complex Formation. *Biomaterials* **2013**, *34* (31), 7653−7661.
(29) Salbach-Hirsch, J.; Samsonov, S. A.; Hintze, V.; Hofbauer, C.; Picke, A.-K.; Rauner, M.; Gehrcke, J.-P.; Moeller, S.; Schnabelrauch, M.; Scharnweber, D.; Pisabarro, M. T.; Hofbauer, L. C. Structural and Functional Insights into Sclerostin-Glycosaminoglycan Interactions in Bone. *Biomaterials* **2015**, *67*, 335.
(30) Wade, R. J.; Burdick, J. A. Engineering ECM Signals into Biomaterials. *Mater. Today* **2012**, *15* (10), 454−459.
(31) Van der Smissen, A.; Hintze, V.; Scharnweber, D.; Moeller, S.; Schnabelrauch, M.; Majok, A.; Simon, J. C.; Anderegg, U. Growth Promoting Substrates for Human Dermal Fibroblasts Provided by Artificial Extracellular Matrices Composed of Collagen I and Sulfated Glycosaminoglycans. *Biomaterials* **2011**, *32* (34), 8938−8946.
(32) Hintze, V.; Miron, A.; Möller, S.; Schnabelrauch, M.; Heinemann, S.; Worch, H.; Scharnweber, D. Artificial Extracellular Matrices of Collagen and Sulphated Hyaluronan Enhance the Differentiation of Human Mesenchymal Stem Cells in the Presence of Dexamethasone. *J. Tissue Eng. Regener. Med.* **2014**, *8*, 314.
(33) Lowry, O. H.; Rosebrough, N. J.; Farr, A. L.; Randall, R. J. Protein Measurement with the Folin Phenol reagent. *J. Biol. Chem.* **1951**, *193* (1), 265−275.
(34) Miron, A.; Rother, S.; Huebner, L.; Hempel, U.; Käppler, I.; Moeller, S.; Schnabelrauch, M.; Scharnweber, D.; Hintze, V. Sulfated Hyaluronan Influences the Formation of Artificial Extracellular Matrices and the Adhesion of Osteogenic Cells. *Macromol. Biosci.* **2014**, *14* (12), 1783−1794.
(35) Farndale, R. W.; Buttle, D. J.; Barrett, A. J. Improved Quantitation and Discrimination of Sulphated Glycosaminoglycans by Use of Dimethylmethylene Blue. *Biochim. Biophys. Acta, Gen. Subj.* **1986**, *883* (2), 173−177.
(36) Balazs, E. A.; Berntsen, K. O.; Karossa, J.; Swann, D. A. An Automated Method for the Determination of Hexosamines. *Anal. Biochem.* **1965**, *12* (3), 559−564.
(37) Van der Harst, M. R.; Brama, P. A. J.; van de Lest, C. H. A.; Kiers, G. H.; DeGroot, J.; van Weeren, P. R. An Integral Biochemical Analysis of the Main Constituents of Articular Cartilage, Subchondral and Trabecular Bone. *Osteoarthr. Cartil.* **2004**, *12* (9), 752−761.
(38) Volpi, N.; Maccari, F.; Titze, J. Simultaneous Detection of Submicrogram Quantities of Hyaluronic Acid and Dermatan Sulfate on Agarose-gel by Sequential Staining with Toluidine Blue and Stains-All. *J. Chromatogr. B: Anal. Technol. Biomed. Life Sci.* **2005**, *820* (1), 131−135.
(39) Altgärde, N.; Nilebäck, E.; De Battice, L.; Pashkuleva, I.; Reis, R. L.; Becher, J.; Möller, S.; Schnabelrauch, M.; Svedhem, S. Probing the Biofunctionality of Biotinylated Hyaluronan and Chondroitin Sulfate by Hyaluronidase Degradation and Aggrecan Interaction. *Acta Biomater.* **2013**, *9* (9), 8158−8166.
(40) Vives, V.; Laurin, M.; Cres, G.; Larrousse, P.; Morichaud, Z.; Noel, D.; Côté, J.-F.; Blangy, A. The Rac1 Exchange Factor Dock5 is Essential for Bone Resorption by Osteoclasts. *J. Bone Miner. Res.* **2011**, *26* (5), 1099−1110.
(41) Maccari, F.; Volpi, N. Glycosaminoglycan Blotting on Nitrocellulose Membranes Treated with Cetylpyridinium Chloride

DOI: 10.1021/acsami.5b08419
ACS Appl. Mater. Interfaces 2015, 7, 23787−23797

after Agarose-gel Electrophoretic Separation. *Electrophoresis* **2002**, *23* (19), 3270−3277.
(42) Freudenberg, U.; Behrens, S. H.; Welzel, P. B.; Müller, M.; Grimmer, M.; Salchert, K.; Taeger, T.; Schmidt, K.; Pompe, W.; Werner, C. Electrostatic Interactions Modulate the Conformation of Collagen I. *Biophys. J.* **2007**, *92* (6), 2108−2119.
(43) Ezzo, J. A. Putting the "Chemistry" Back into Archaeological Bone Chemistry Analysis: Modeling Potential Dietary Indicators. *Journal Of Anthropological Archaeology.* **1994**, *13*, 1−34.
(44) Lemmnitzer, K.; Schiller, J.; Becher, J.; Möller, S.; Schnabelrauch, M. Improvement of the Digestibility of Sulfated Hyaluronans by Bovine Testicular Hyaluronidase: A UV Spectroscopic and Mass Spectrometric Study. *BioMed Res. Int.* **2014**, *2014*, 1.
(45) Bierbaum, S.; Douglas, T.; Hanke, T.; Scharnweber, D.; Tippelt, S.; Monsees, T. K.; Funk, R. H. W.; Worch, H. Collageneous Matrix Coatings on Titanium Implants Modified with Decorin and Chondroitin Sulfate: Characterization and Influence on Osteoblastic Cells. *J. Biomed. Mater. Res., Part A* **2006**, *77* (3), 551−562.
(46) Douglas, T.; Heinemann, S.; Mietrach, C.; Hempel, U.; Bierbaum, S.; Scharnweber, D.; Worch, H. Interactions of Collagen Types I and II with Chondroitin Sulfates A-C and their Effect on Osteoblast Adhesion. *Biomacromolecules* **2007**, *8* (4), 1085−1092.
(47) Tian, H.; Li, C.; Liu, W.; Li, J.; Li, G. The Influence of Chondroitin 4-sulfate on the Reconstitution of Collagen Fibrils In Vitro. *Colloids Surf., B* **2013**, *105*, 259−266.
(48) Van der Smissen, A.; Samsonov, S.; Hintze, V.; Scharnweber, D.; Moeller, S.; Schnabelrauch, M.; Pisabarro, M. T.; Anderegg, U. Artificial Extracellular Matrix Composed of Collagen I and Highly Sulfated Hyaluronan Interferes with TGFβ(1) Signaling and Prevents TGFβ(1)-induced Myofibroblast Differentiation. *Acta Biomater.* **2013**, *9* (8), 7775−7786.
(49) Wood, G. C.; Keech, M. K. The Formation of Fibrils from Collagen Solutions. 1. The Effect of Experimental Conditions: Kinetic and Electron-microscope Studies. *Biochem. J.* **1960**, *75*, 588−598.
(50) Obrink, B. The Influence of Glycosaminoglycans on the Formation of Fibers from Monomeric Tropocollagen In Vitro. *Eur. J. Biochem.* **1973**, *34* (1), 129−137.
(51) Stamov, D.; Grimmer, M.; Salchert, K.; Pompe, T.; Werner, C. Heparin Intercalation into Reconstituted Collagen I Fibrils: Impact on Growth Kinetics and Morphology. *Biomaterials* **2008**, *29* (1), 1−14.
(52) Stuart, K.; Panitch, A. Influence of Chondroitin Sulfate on Collagen Gel Structure and Mechanical Properties at Physiologically Relevant Levels. *Biopolymers* **2008**, *89* (10), 841−851.
(53) Gatej, I.; Popa, M.; Rinaudo, M. Role of the pH on Hyaluronan Behavior in Aqueous Solution. *Biomacromolecules* **2005**, *6* (1), 61−67.
(54) Phan, T. C. A.; Xu, J.; Zheng, M. H. Interaction between Osteoblast and Osteoclast: Impact in Bone Disease. *Histol. Histopathol.* **2004**, *19* (4), 1325−1344.
(55) Lee, C. W.; Seo, J. Y.; Choi, J. W.; Lee, J.; Park, J. W.; Lee, J. Y.; Hwang, K. Y.; Park, Y. S.; Park, Y., Il. Potential Anti-osteoporotic Activity of Low-molecular Weight Hyaluronan by Attenuation of Osteoclast Cell Differentiation and Function In Vitro. *Biochem. Biophys. Res. Commun.* **2014**, *449* (4), 438−443.
(56) Ariyoshi, W.; Takahashi, T.; Kanno, T.; Ichimiya, H.; Takano, H.; Koseki, T.; Nishihara, T. Mechanisms Involved in Enhancement of Osteoclast Formation and Function by Low Molecular Weight Hyaluronic Acid. *J. Biol. Chem.* **2005**, *280* (19), 18967−18972.
(57) Ariyoshi, W.; Okinaga, T.; Knudson, C. B.; Knudson, W.; Nishihara, T. High Molecular Weight Hyaluronic Acid Regulates Osteoclast Formation by Inhibiting Receptor Activator of NF-κB Ligand through Rho Kinase. *Osteoarthr. Cartil.* **2014**, *22* (1), 111−120.
(58) Baud'huin, M.; Ruiz-Velasco, C.; Jego, G.; Charrier, C.; Gasiunas, N.; Gallagher, J.; Maillasson, M.; Naggi, A.; Padrines, M.; Redini, F.; Duplomb, L.; Heymann, D. Glycosaminoglycans Inhibit the Adherence and the Spreading of Osteoclasts and their Precursors: Role in Osteoclastogenesis and Bone Resorption. *Eur. J. Cell Biol.* **2011**, *90* (1), 49−57.
(59) Ariyoshi, W.; Takahashi, T.; Kanno, T.; Ichimiya, H.; Shinmyouzu, K.; Takano, H.; Koseki, T.; Nishihara, T. Heparin Inhibits Osteoclastic Differentiation and Function. *J. Cell. Biochem.* **2008**, *103* (6), 1707−1717.

DOI: 10.1021/acsami.5b08419
ACS Appl. Mater. Interfaces 2015, 7, 23787−23797